Article

Landscape Evolution Modelling of a Post-mining Catchment for Long-term Simulations

Devika Nair [1,2,*], K G Evans [2,3] and Sean Bellairs [1,2]

[1] Research Institute for Environment & Livelihoods, Charles Darwin University, Ellengowan Drive, Casuarina, NT 0810, Australia; sean.bellairs@cdu.edu.au
[2] College of Engineering, IT & Environment, Charles Darwin University, Ellengowan Drive, Casuarina, NT 0810, Australia; ken.evans@swesolutions.com.au (K.G.E.)
[3] Surface Water & Erosion Solutions, Lakes Crescent, Marrara, NT 0812, Australia.
* Correspondence: devika.nair@cdu.edu.au

Abstract: Landform Evolution Modelling (LEM) provides an avenue for simulating how a landscape may evolve over extended time periods of thousands of years. The CAESAR-Lisflood LEM that includes a hydrologic model (TOPMODEL) and a hydraulic model (Lisflood) can be used to assess the proposed final landform morphology of a mine site by simulating how the mine landform and the landscape would evolve over a 1,000-year period. The accuracy of future simulations depends on the calibration and validation of the model to the past and present events. Calibration and validation of the model involves finding a combination of parameters of the model which when applied and simulated gives model outputs similar to those observed for the real site scenario for corresponding input data. Calibrating the sediment output of the CAESAR-Lisflood model at the catchment level and using it for studying the equilibrium conditions of the landform is an area yet to be explored. Therefore, the aim of this study was to calibrate the CAESAR-Lisflood model and then validate it. To achieve this, the model was run for a rainfall event with a set of parameters, plus discharge and sediment data for the input point of the catchment, to analyze how similar the model output would behave when compared with the discharge and sediment data for the output point of the catchment. The model parameters were then adjusted until the model closely approximate the real site values of the catchment. It was then validated by running the model for a different set of events and checking that the model gave similar results to the real site values. The outcomes demonstrated that while the model can be calibrated to a greater extent for hydrology (discharge output) throughout the year, the sediment output calibration may be slightly improved by having the ability to change parameters to take into account the seasonal vegetation growth during the start and end of the wet season. This study is important for designing and testing post-mining rehabilitated landscape systems that assess hydrology and sediment movement in seasonal biomes.

Keywords: Landform evolution modelling; catchment hydrology; post-mining landscape; sediment transport; mine rehabilitation

1. Introduction

Minescapes are landscapes generated by mining activity, and most of the research and literature on the subject has focused on geomorphologically based assessments of mining-affected catchments. Mining operations cause a significant environmental disturbance, and if not managed appropriately, may have detrimental impacts in the future. They may potentially disturb large areas of the land surface well beyond the area directly affected. Post-mining the operators are usually required to return the landscape to a geomorphically stable system that integrates with its surroundings. Often these reconstructed landscapes contain uneconomic ore, mine processing waste and in the case of uranium mines, low-grade uranium and associated fines from the mineral extraction process. These environmentally hostile materials are required to be encapsulated within the structure for

 doi:10.20944/preprints202306.1072.v1

millennia [1]. Thus, the rehabilitation of mine landforms to a stable state is of paramount importance.

One of the main challenges in studies pertaining to mine rehabilitation is the need to assess how a landform may evolve under different site conditions and rehabilitation initiatives. Since geomorphological processes are very slow, the assessment of landform evolution may be done over an extended time of thousands of years. Landscape Evolution Modelling (LEM) provides an avenue for simulating how a landscape may evolve over extended time periods of thousands of years.

During landform disturbances such as mining, there will be sediment spikes in receiving waters during rainfall events. Then, as the rehabilitated site approaches equilibrium with the surrounding catchment, the sediment spikes for a given discharge should return to pre-mining levels. Once this is achieved, a landform may be considered stable [2].

Thus, to examine the dynamics of landform stability in future years, a landform evolution model could be used to simulate discharge and corresponding sediment output in the catchment where the mine resides, to assess when elevated spikes due to mining disturbance no longer occur [3].

To use CAESAR- Lisflood LEM and to examine the dynamics of landform stability in the catchment where the Ranger mine resides, initially, the model would have to be calibrated and validated for past events. There has been a previous study where the CAESAR-Lisflood LEM had been modelled for trial landform at Ranger mine for specific site hydrological conditions and sediment loads, and it demonstrated excellent agreement with the field data from experimental erosion plots at Ranger mine trial landform [4].

This study encompassed modelling of the whole Gulungul catchment where the Ranger mine resides and then calibrating and validating the hydrology and sediment transport in the stream flow of the catchment. This paper focused on (1) calibrating the CAESAR- Lisflood LEM model for observed hydrology and sediments; (2) running this calibrated model for one year to validate it and (3) examining whether the calibrated Manning's n values varied between the start and end of the wet season.

2. Site Description

Ranger mine (12°41′ S, 132°55′ E) is an open cut uranium mine operated by Energy Resources of Australia Ltd. (ERA) in Northern Territory, Australia. The mine is located 8 km east of the township of Jabiru and within the 78 km^2 Ranger Project Area which is surrounded by, but separate from, the World Heritage-listed Kakadu National Park (Figure 1). It has been producing uranium oxide (U_3O_8) since 1981 and is presently undergoing rehabilitation and closure. Mining ceased in 2012, milling of the mined ore ceased in early 2021 and work is now focused on rehabilitation [5].

The regional geology around the Ranger mine is dominated by the mineralised metasediments and igneous rocks of the Pine Creek geosyncline and the younger sandstones of the Mamadawerre Formation. The Ranger site is characterised geomorphically as part of the deeply weathered Koolpinyah surface. This consists of plains, broad valleys, and low gradient slopes, with isolated hills and ridges of resistant rock [6]. Located in the monsoon tropics, the Ranger mine experiences a distinct wet season from October to April and a dry season for the remainder of the year. Consequently, streamflow is highly seasonal. The average annual rainfall is 1,557 mm [7].

The unique location of the Ranger mine in the Northern Territory of Australia, surrounded by the World Heritage– listed Kakadu National Park and upstream of floodplains and wetlands listed as Wetlands of International Significance under the Ramsar Convention, has meant that significant environmental and cultural sensitivity surrounds the operation of the mine and its pending closure and rehabilitation. Consequently, increasing focus has been on the development of appropriate closure criteria and rehabilitation plans for the mine [8]. ERA is responsible for the rehabilitation of Ranger mine based on laid out principles called Environmental Requirements (ERs). The Supervising

Preprints (www.preprints.org) | NOT PEER-REVIEWED | Posted: 15 June 2023 doi:10.20944/preprints202306.1072.v1

Scientist has supervisory role. ERs pertaining to erosion equilibrium of the landform require erosion characteristics which, as far as can reasonably be achieved, do not vary significantly from those of comparable landforms in surrounding undisturbed areas. It is expected that the erosion rates will initially be high then tend slowly towards the natural rates. These timeframes are expected to be quite long so the outcome is to use best available modelling to demonstrate that the erosion characteristics of the final landform will eventually be comparable to natural landscapes.

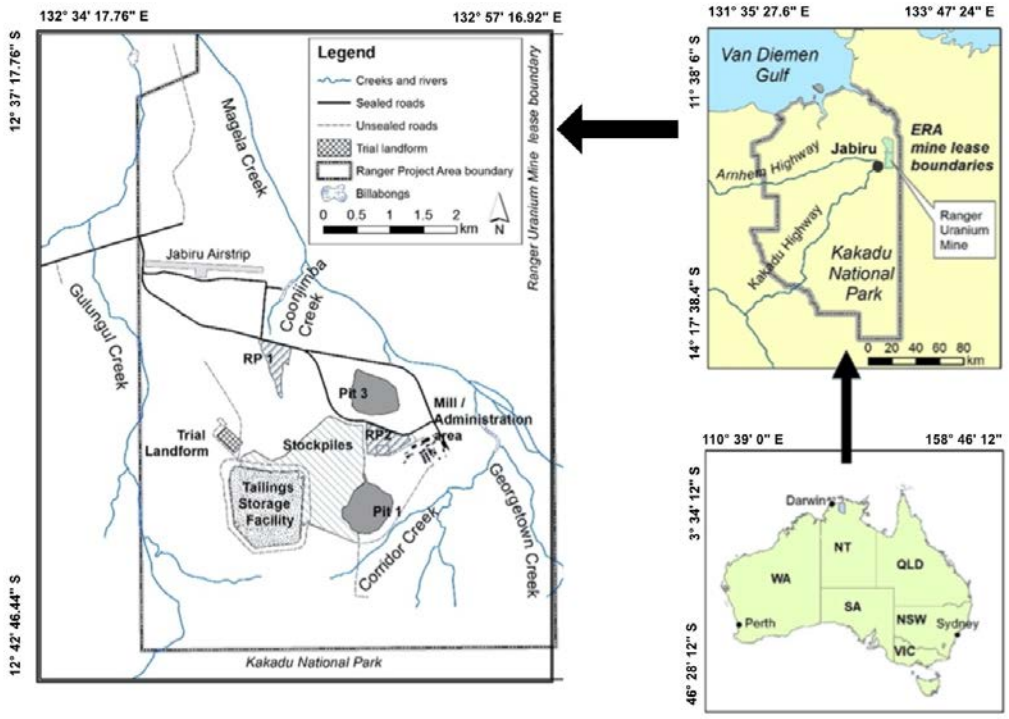

Figure 1. Location of Ranger Uranium Mine. Adapted from Lowry et al. (2020) and reproduced under Creative Commons CC by attribution.

The Ranger mine is adjacent to Magela Creek, a left-bank tributary of the East Alligator River [5]. Gulungul Creek is a small tributary of Magela Creek that is adjacent to the tailings dam. It is one of the tributaries that would be the first to receive sediment generated from the mine site during and after rehabilitation [9]. Gulungul and Magela Creeks are ephemeral sand-bed braided streams which carry very large sand loads (bed and suspended bed) and small FSS (fine suspended sediment) loads. Environmental Research Institute of the Supervising Scientist (eriss) had monitoring sites in Gulungul Creek downstream (GCDS), Gulungul Creek upstream (GCUS), Magela Creek downstream (MCDS), and Magela Creek upstream (MCUS) of the mine (Figure 2). The data obtained from eriss for this study were continuous discharge (m^3), and turbidity (NTU) and FSS (<63 µm fraction of sediment samples collected in the auto-samplers; mg). Data were from August 2004 to August 2015 measured at a frequency of 6 min for Gulungul Creek GCDS and GCUS. Rainfall data for GCDS and GCUS at 10 min interval were also obtained for modelling Gulungul catchment in CAESAR-Lisflood.

Preprints (www.preprints.org) | NOT PEER-REVIEWED | Posted: 15 June 2023 doi:10.20944/preprints202306.1072.v1

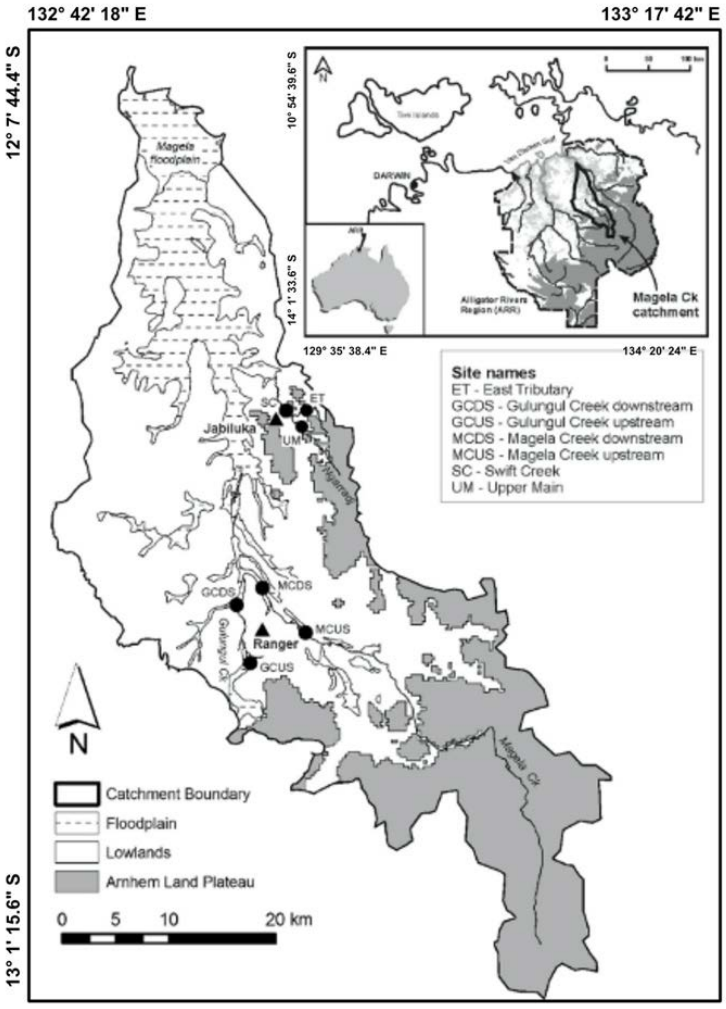

Figure 2. Location of gauging stations at Ranger. Adapted from Moliere and Evans (2010); copyright Commonwealth of Australia.

3. Landform Evolution Modelling

Numerical landscape evolution models (LEMs) are tools that may be used to examine the geomorphic behaviour of landscapes through incorporating factors such as pedogenesis, climate, geology, and vegetation growth. They can operate over time scales ranging from years to millennia, and spatial scales from sub hectare to entire regions [10]. Models to predict surface stability can be placed in two broad categories: (1) soil loss prediction or soil erosion models and (2) topographic evolution models [11].

Soil loss prediction or soil erosion models have typically been developed for agricultural purposes, but some of the soil loss prediction models that can be applied to mining landforms are RULSE, CREAMS, WEPP [12].

Topographic Evolution Models (TEM) or Landscape Evolution Models (LEM) are process-response models based on modelling erosion and accumulation of material over time across a landform. They give an indication of the long-term geomorphological development of a formed surface subjected to erosion and deposition processes [11]. They can also be used to predict the development of drainage problem areas and gullies. Early models [13] simply modelled where aggradation occurred (when more material entered an area than was removed) and where net erosion occurred (where less material entered an area than was removed). Advances in computing technology now allow this concept to be applied to nodes on a digital terrain map (DTM). This concept allows 3-D graphic representation of simulations by recently developed models.

 doi:10.20944/preprints202306.1072.v1

SIBERIA is a sophisticated 3-D TEM that simulates both runoff and erosion and it predicts the long-term evolution of channels and hillslopes in a catchment [14]. Initial modelling of Ranger mine focused on using SIBERIA and CAESAR LEMs to determine whether the uranium remaining in the waste rock would remain buried for 10,000 years. Landform evolution modelling (LEM) methods were developed through a significant amount of research including: field programs using plot and catchment studies to calibrate sediment transport and hydrology models for the calibration of the Siberia LEM and assessing mine landform stability over a 1000 y period; using catchment denudation rates, empirical modelling and numerical modelling to assess the Ranger landform design; field studies to assess the temporal change in Siberia parameter values as a landscape matures; assessing the impact of extreme rainfall events in the Ranger landform using CEASAR-Lisflood; simulating long term (up to 10,000 y) erosion, on the Ranger landform; the effects of climate change; comparison of the undisturbed Magela Creek catchment and the mine-disturbed catchment using CAESAR-Lisflood simulations; and large scale trial landform studies [2].

Till 2008, the Siberia LEM was the only geomorphic computer modelling code being used to predict the long-term behavior of the Ranger rehabilitated landform. Siberia simulations use as input an average area-discharge relationship for a wet season and do not use the time series hydrology of a single rainfall event or series of events. Consequently, the average long-term erosion assessments conducted to date have not implicitly addressed the impact of an extreme rainfall event or a series of events comprising an 'extreme' wet season. CAESAR [15] was introduced since it features slope processes (soil creep, mass movement), hydrological processes, multidirectional routing of river flow and fluvial erosion and deposition over a range of different grain sizes. A tracing component allows input of contaminant data to assess transport downstream. This is especially important because it enables routing of sediment lost from the landform through a river catchment. Such functionality is not present in Siberia. CAESAR-Lisflood LEM was used in this study as it works at much finer temporal resolution than SIBERIA.

3.1. CAESAR-Lisflood LEM

CAESAR-Lisflood [16, 17] includes a hydrologic model (TOPMODEL) and a hydraulic model (Lisflood). It simulates landscape development by routing water over a regular grid of cells and altering elevations of individual cells according to numerically calculated erosion and deposition rates from fluvial and slope processes. Runoff over the landform is generated through the input of rainfall data using an adaptation of TOPMODEL [18]. Surface flow is routed using Lisflood-FP [19], a two-dimensional hydrodynamic flow model. Morphological changes to the landform result from transport and deposition of sediments. Einstein (1950) and Wilcock and Crowe (2003) sediment transport equations are the two options for calculating sediment transport in this version of CAESAR-Lisflood model [20, 21].

A key attribute of the CAESAR-Lisflood model is the ability to use variable time-interval rainfall data from the study area. This enables modelling of the effects of specific rainfall events. As the climatic region in which the Ranger mine occurs is dominated by seasonal, high-intensity rainfall events, the ability to model specific rainfall events means that the CAESAR-Lisflood model is the most suitable model for this study.

CAESAR can be used to simulate the impact of extreme rainfall events, since time series data for actual or simulated rainfall events can be used as input. This ability is a critical attribute given the long times that radioactive material is required to be contained, and the probability that one or more very extreme rainfall events will occur. Extreme event testing of the proposed design parameters for the constructed landform has assumed greater importance given the possibility of an increase in frequency of intense rainfall periods because of climate change.

The CAESAR-Lisflood LEM requires three key data inputs: a digital elevation model of the landform, rainfall data, and particle size distribution data of the landform surface.

Preprints (www.preprints.org) | NOT PEER-REVIEWED | Posted: 15 June 2023 doi:10.20944/preprints202306.1072.v1

The presence or absence of a vegetation cover may also be incorporated into model simulations.

The parameters for CAESAR-Lisflood used in this study are given in Table 1. The particle size distribution (grain sizes and corresponding proportions) for the watershed is taken from Evans (2022) [22]. Suspended sediment particle sizes are the mud and clay component (<63 μm fraction sediments) of the soil. There are three sediment transport equations available in CAESAR-Lisflood namely Wilcock and Crow, Einstein and Mayer Peter Muller. Wilcock and Crow sediment transport equation (equation 1) was used for modelling since it gave reasonable results comparable to field data in this study. The transport potential of Wilcock and Crow (2003) formla is given by:

$$q_{bk} = u^3 * W_k / R_k g \quad (1)$$

where, q_{bk} = fractional bed-load sediment transport potential [L^2/T], u = bed shear velocity [L/T], W_k = transport function, $R_k = \varrho_{sk}/\varrho_w - 1$ = submerged specific gravity of grain class, ϱ_{sk} = sediment grain density [M/L^3], ϱ_w = water density [M/L^3], g = gravitational constant [L/T^2] [21]. The fall velocity of suspended sediment is 0.026 m/s for 63 μm fraction sediments. Manning's 'n' and 'm' values in the parameters are calibrated values. Description of Manning's n value selection are detailed in Section 7. According to Bureau of Meteorology data, the average annual evaporation rate is 2000mm in Ranger mine area. Thus the daily evaporation rate in the watershed is given as 0.0055m/day [23]. Maximum erode limit of the catchment is given as 0.02m for calibration and thus the active layer thickness which should be more than four time the maximum erode limit is given as 0.1m. Input/output difference is the minimum value of input for which the model gives output. It is given as 0 m^3/s. All the other parameters in the model are taken as default values.

Table 1. CAESAR-Lisflood Parameters.

CAESAR-Lisflood Parameters	Values
Grainsizes (m)	0.000063, 0.001, 0.002, 0.004, 0.008, 0.016, 0.032, 0.064, 0.128
Grainsize proportions (corresponding to above sizes)	0.144, 0.022, 0.019, 0.029, 0.068, 0.146, 0.220, 0.231, 0.121
Sediment transport law	Wilcock & Crow
Max erode limit (m)	0.02
Active layer thickness (m)	0.1
m value	0.1
Input/output difference ($m^3\ s^{-1}$)	0
Evaporation rate (m/day)	0.0055
Manning's n (Waste rock, stream, riparian zone, swale, savannah woodlands)	0.02, 0.06, 0.07, 0.03, 0.04

4. Catchment Digital Elevation Model

The DEM used in this study was a 10m resolution digital elevation model of Gulungul catchment obtained from eriss. The catchment area of 25 km^2 encompasses the Gulungul creek and parts of Ranger mine with the waste rock dump and the trial landform (Figure 3). The eriss monitoring sites at GCUS and GCDS record rainfall, discharge, and turbidity. These data were used for calibration and validation of the model.

5. Rainfall Data

Rainfall data input into CAESAR-Lisflood was hourly data from eriss. Rainfall data at 10 min intervals from 2005 to 2015 for GCUS and GCDS were obtained from eriss. There are two other BOM (Bureau of Meteorology) stations nearby Gulungul catchment where rainfall data are available that would influence parts of the catchment. They are the Jabiru

 doi:10.20944/preprints202306.1072.v1

Airport and Jabiru Fire station (Figure 4). Half-hourly rainfall data for Jabiru airport/fire station was obtained from BOM from 2005 to 2015. Use of data from a number of gauging stations gave more accurate hourly discharge modeling results during hydrology calibration. Thus, four gauging station data were used in this study.

The model was initially calibrated for a rainfall event from 25th December 2011 to 28th December 2011. The rainfall data of all four stations were converted to hourly rainfall intensity (mm) for that time period, and the text file of the rainfall data was used as input in the hydrology tab of the model.

Voronoi polygons were drawn in the Quantum geographic information system (QGIS) [24] for the four stations to determine the area of influence of each rainfall station and these areas were clipped to Gulungul catchment polygon as shown in Figure 4. The catchment was divided into four sections where each of the station's rainfall data were input. Thus, the Voronoi polygons in Figure 4 depicted how the rainfall from four different rain gauges were spatially distributed in the catchment. The rasterized file of this DEM in *.ASC format was input into the hydroindex file in the hydrology tab of the model.

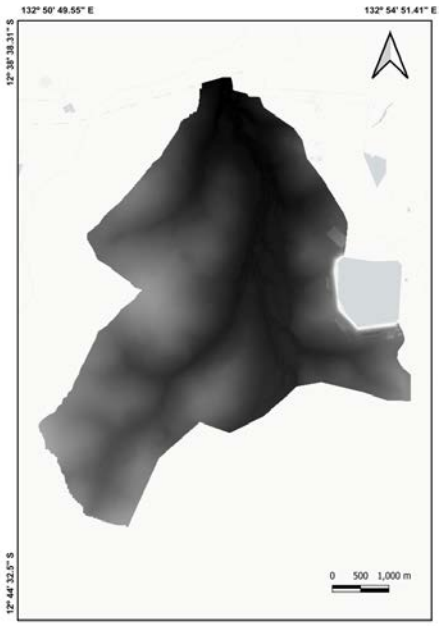

Figure 3. Digital Elevation Model of Gulungul Catchment,.

Preprints (www.preprints.org) | NOT PEER-REVIEWED | Posted: 15 June 2023 doi:10.20944/preprints202306.1072.v1

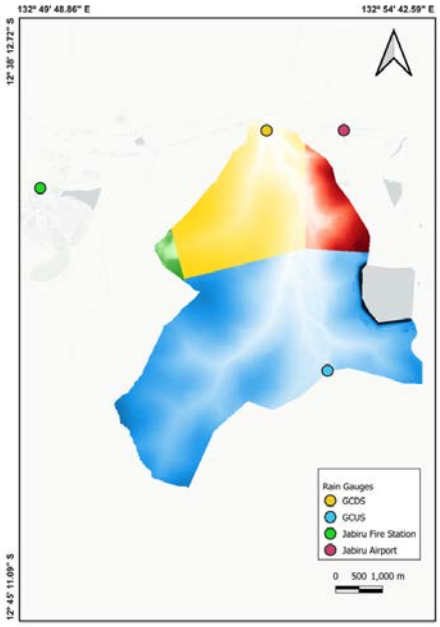

Figure 4. Rainfall Stations and their influence areas in Gulungul Catchment.

6. Input Discharge and Sediment

The input file was a text file with fourteen columns, where- each row was one input time step (each time step was 1 hour). The fourteen columns were time, discharge (m^3s-1), three blank columns, nine columns with the volumes in m^3 of sediment for each of the nine separate grain size fractions specified in the sediment tab of the model. The last column was the volume of FSS.

Catchment input discharge (m^3s^{-1}) for Gulungul Creek at GCUS in 6 min intervals was obtained from eriss. Discharge data was averaged to get hourly discharge at GCUS in m^3s^{-1}.

The turbidity can be used as a surrogate measure of observed FSS load [25]. A site specific relationship between FSS and turbidity for GCUS was developed for this study by Nair et al. (2021) [2]. To estimate FSS, turbidity data (NTU) for Gulungul Creek at GCUS in 6 min intervals was obtained from eriss. The relationship by Nair et al. (2021) was used to find the volume of FSS (m^3) load corresponding to hourly discharge (Table A1). Volume of sediment of the remaining eight separate grain sizes were required for the input text file. Since there was no available observed data for bedload for each of these grain sizes during the calibration event period, bed load was quantified using a site-specific relationship between bedload and total sediment load.

The site specific relationship between total sediment load and bedload is [26]

$$\text{Total sediment load} = 1.28 * \text{bedload}^{1.02} \quad (2)$$

(r^2=0.99, p<0.001)

Particle size analysis data is available for GCUS during 2007-2008 from eriss. This gives the quantity of bedload sediment corresponding to respective grain sizes. Equation 2 can be used to find total sediment load in one of the above data sets and the difference between total sediment load and bedload gives total suspended load (total suspended sand + total suspended mud). The proportion of suspended sand to suspended mud for the catchment is 41:28 [27] . Further data and calculations are shown in Table A2 and A3. Using the above data, the weight of total sediment of each grain size was determined. The proportion of sediments of each grain size was thus determined and used to find the volume of sediments of separate grain sizes for the calibration rainfall event (Table A4). The resulting text input file was entered into the reach input variable of the hydrology tab in the CAESAR-Lisflood model.

 doi:10.20944/preprints202306.1072.v1

7. Manning's n Values

Manning's coefficient 'n' depicts the level of surface roughness affecting flow velocity and flow path. Manning's n [28] is formulated as:

$$n = (1/v)*(R)^{2/3}*(S)^{1/2} \quad (3)$$

where v is average velocity in ms^{-1}, R is hydraulic radius in m and s is slope of the channel at the point of measurement. The chainage distances from the banks across the creek with the corresponding depth of the creek and velocity of flow data from eriss for Gulungul Creek was used to find Manning's n using equation 3. The slope of the channel was determined from DEM using GIS. The value was found to be around 0.06 across the stream. There are different areas on Gulungul catchment based on vegetation and soil types depicting different roughness co-efficients or Manning's n values. The catchment polygon was divided into different polygons namely waste rock, stream, riparian zone, swale and savanna woodlands (Figure 5). This was mapped in GIS software using satellite imagery of the catchment. The shape file of the catchment and Manning's polygon was overlapped, and the rasterized file was imported to flow model tab of CAESAR-Lisflood model. Stream was given 'n' value of 0.06 and other areas were given values based on Chow (1959) [29]. There are a range of values that could be used to each of the polygons divided based on their vegetation and soil types and these values along with other parameters of the model were adjusted during calibration. Use of different Manning's n values based on land cover and vegetation depicts more realistic depiction of the watershed.

8. Results

8.1. Model Calibration

The Gulungul catchment was studied to return to back ground erosion levels in 2011 wet season after the disturbance caused by trial landform construction in 2008 in Ranger mine [2]. Thus, a relatively large individual storm event in 2011 wet season was selected for model calibration [30]. The model was calibrated to observed hydrology and sediment output at GCDS for a rainfall event from 25th December 2011 to 28th December 2011. All the input data were sorted as described in the above sections and the model was run to get an output (catchment.dat) file. For a specified time, the output file contains fourteen columns: time, Qw (actual), Qw (expected), a blank column, total sediment output in time step (m^3), followed by nine columns that have the volumes in m^3 of sediment for each of the nine separate grain size fractions. The time interval for the output in this study is hourly (same as the input).

Modelled discharge and FSS data from the output file were compared with the observed data at GCDS. In the CAESAR-Lisflood model, set of Manning's coefficient 'n' (level of surface roughness affecting flow velocity and flow path) and the hydrograph exponent 'm' (determines the peakiness and duration of the hydrograph) was adjusted so that the predicted discharge hydrograph and event FSS quantity were similar to the observed values. While calibrating, the best fit was determined by selecting the set of values for Manning's 'n' and hydrograph exponent 'm' such that the modelled event FSS quantity is approximately same as observed event FSS quantity and the modelled hydrology peak and duration is similar to the observed through visual assessment. Hydrology peak (Figure 6a) and event sediment quantity were calibrated (Figure 6b) with Manning's n values of stream =0.06, swale = 0.03, riparian zone = 0.07, savannah woodlands = 0.04 and waste rock =0.02; hydrology exponent 'm' = 0.01. Total event FSS quantity for an event discharge was considered during calibration of the model since the model is calibrated for future simulations to predict future FSS quantity during rainfall events [2].

Preprints (www.preprints.org) | NOT PEER-REVIEWED | Posted: 15 June 2023 doi:10.20944/preprints202306.1072.v1

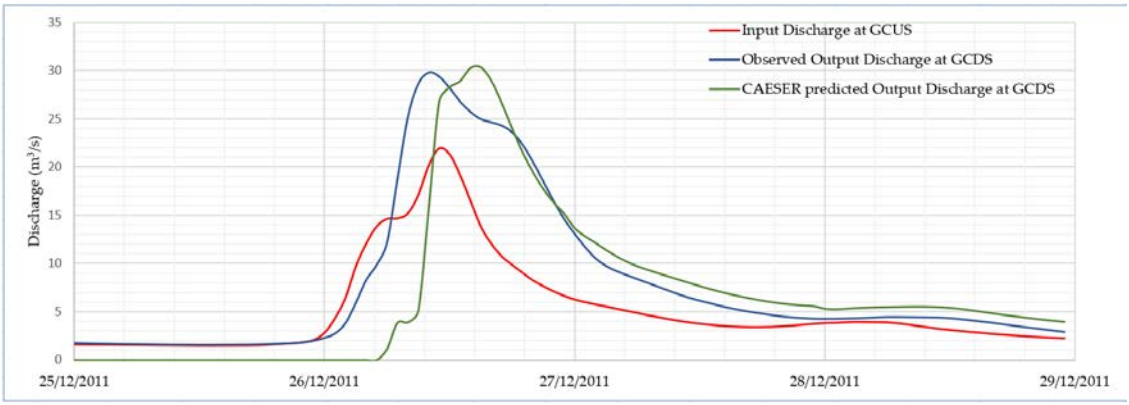

Figure 6a. Calibration Results comparing the observed output discharge with model outputs.

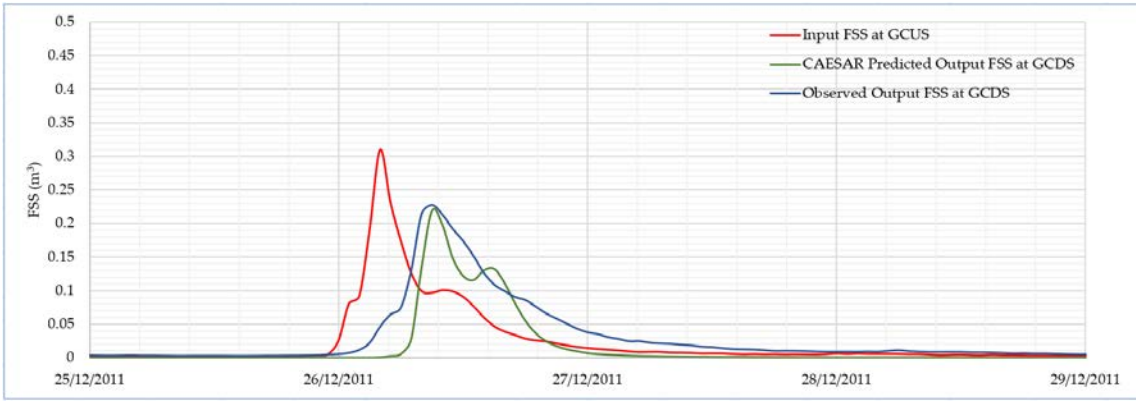

Figure 6b. Calibration Results comparing the FSS quantities with model outputs.

8.2. Model Validation

The model was run with calibrated parameters for a whole year encompassing the rainfall event used for calibration. Data for input discharge, rainfall at all four rainfall stations and sediment volume for different grain sizes were sorted for hourly input from August 31st, 2010 to August 31st, 2011. Since the model was run for a year, rainfall initial loss (400 mm) and continuous loss (2.4 mm/h) was reduced from the total rainfall [31]. The initial loss defines the volume of water that is required to fill the soil layer at the start of the simulation and continuous loss defines the rate at which precipitation will be infiltrated into the soil layer after the initial loss volume has been satisfied.

Model hydrology was validated since the CAESAR-Lisflood discharge output at GCDS was similar to observed hydrology in terms of peak and duration of the hydrograph (Figure 7a) for the whole year. Regarding the sedigraph, the model simulated FSS spikes similar to observed data at GCDS for the start of the wet season (Figure 7b). Towards the end of wet season, CAESAR-Lisflood underpredicted the observed FSS spikes. The start of wet season in 2011 on the Ranger mine site is estimated as October 9, 2011 and end of wet season as April 9, 2012 (Segura Pers. Comm.). The start and end of wet season was considered based on plant available water (PAW). Initial rise in PAW which was sustained was marked as start of wet season and date after which PAW consistently declined was considered the end of wet season. The reason behind the model underpredicting event FSS quantity may be due to change in vegetation ground cover and evapotranspiration towards the second half of the wet season. The ground cover vegetation is strongly seasonal with vigorous grass growth during the wet season and a substantial decline in grass foliage cover during the dry season. Most transpiration occurs from the grassy ground cover rather than from the trees, and ground cover transpiration is minimal at the start of the wet season but high during the middle to the end of the wet season [32].

Preprints (www.preprints.org) | NOT PEER-REVIEWED | Posted: 15 June 2023 doi:10.20944/preprints202306.1072.v1

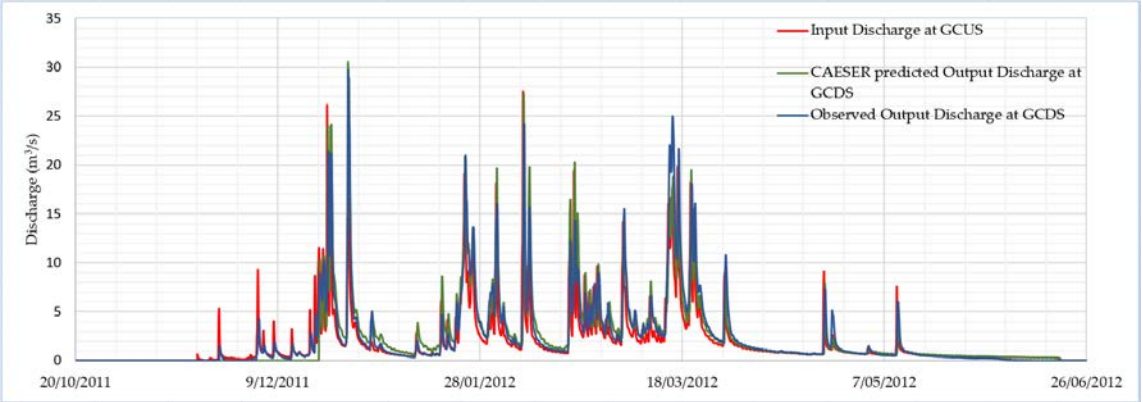

Figure 7a. Validation Results comparing the observed output discharge and FSS quantities with model outputs.

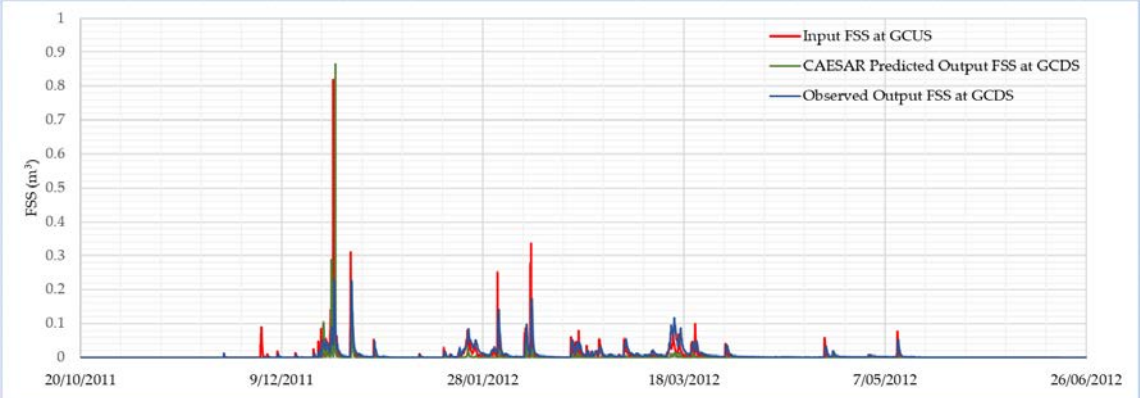

Figure 7b. Validation Results comparing the observed FSS quantities with model outputs.

9. Conclusion

Calibrating and validating the model with variable input parameters gives an insight to how sensitive CAESAR-Lisflood is to each parameter. The model was run using different combinations of Manning's 'n' and hydrology exponent 'm' to calibrate the hydrology and event sediment quantity to the observed values at catchment output. While hydrology could be easily calibrated with 'm' = 0.01 and a range of Manning's 'n' values over the catchment; sediment event output quantity narrowed the range of 'n' values that could be used to calibrate the model for the catchment. Using variable Manning's n values over the catchment based on an ecological map based on soil type and vegetation community instead of a single value of n for the entire catchment is a more realistic depiction of site scenario.

The sedigraph peak and event sediment quantity could not be calibrated together for the same values of Manning's 'n'. This may be because the sediment values were computed from turbidity values using a linear equation relating suspended sediment quantity and its' corresponding turbidity. The equation was statistically generated with values taken over number of years and thus the equation represents an average situation where an individual event sediment peak may deviate from the actual. However, in this study the model was calibrated to observed event sediment quantity since this value was required to check the landform stability for future simulations.

During validation, the Manning's 'n' values that accurately calibrate event sediment quantity during the start of wet season were inaccurate at the end of the season. From the second half of the wet season, a different set of Manning's 'n' values were required for accurate event sediment quantity calibration of the model. There are substantial changes in catchment vegetation and changes in soil properties (i.e. increased organic content) over

Preprints (www.preprints.org) | NOT PEER-REVIEWED | Posted: 15 June 2023 doi:10.20944/preprints202306.1072.v1

the wet season. If the changing vegetation could be directly accounted for in the model, the validated model could be run for future simulations to determine event sediment quantity for a corresponding discharge and thus understand landscape equilibrium dynamics.

Future work pertaining to the study includes generation of long-term rainfall scenarios using climate records and global climate models. The modelled catchment along with long-term rainfall scenarios facilitates prediction of discharge and sediment output for predicted wet and dry rainfall scenarios. This helps determining the dynamics of landform evolution of the catchment over the years post-mining.

Author Contributions: Conceptualization: K.E and D.N.; methodology: K.E and D.N; formal analysis: K.E, D.N and M.R.N.; writing—original draft preparation: D.N & K.E.; writing—review and editing: D.N,K.E and S.B.; project administration: K.E. All authors have read and agreed to the published version of the manuscript.

Funding: This research received no external funding.

Data Availability Statement: Not Applicable.

Acknowledgments: The Environmental Research Institute of the Supervising Scientist (eriss) is thanked for the provision of the data for this study. Professor Ken Evans's time was provided by Surface Water & Erosion Solutions as an in-kind contribution.

Conflicts of Interest: The authors declare no conflict of interest.

Appendix A

Table A1. Calculations to determine hourly FSS volume (m3) from observed turbidity data.

Hourly Turbidity in NTU (observed data)	Hourly Turbidity in mg/L (using turbidity-FSS relationship)	Hourly discharge in m^3s^{-1} (observed data)	Hourly discharge in L	Hourly sediment output in mg (Hourly discharge in L*Hourly Turbidity in mgL^{-1})	Hourly sediment output in kg	Hourly sediment output in m^3 (Density = 2650 kgm^{-3})
2	1.04	1.569691	5650887.6	5876923.104	5.876923	0.002217707
2	1.04	1.55642	5603112	5827236.48	5.827236	0.002198957
1.94	1.0088	1.550194	5580698.4	5629808.546	5.629809	0.002124456
1.9	0.988	1.54398	5558328	5491628.064	5.491628	0.002072312
1.9	0.988	1.537784	5536022.4	5469590.131	5.46959	0.002063996
1.84	0.9568	1.527378	5498560.8	5261022.973	5.261023	0.001985292
1.83	0.9516	1.521929	5478944.4	5213763.491	5.213763	0.001967458
1.87	0.9724	1.51062	5438232	5288136.797	5.288137	0.001995523
1.76	0.9152	1.503162	5411383.2	4952497.905	4.952498	0.001868867
1.82	0.9464	1.495728	5384620.8	5096005.125	5.096005	0.001923021
1.85	0.962	1.484442	5343991.2	5140919.534	5.14092	0.00193997
1.87	0.9724	1.47205	5299380	5153117.112	5.153117	0.001944572
1.7	0.884	1.461762	5262343.2	4651911.389	4.651911	0.001755438
1.88	0.9776	1.460458	5257648.8	5139877.467	5.139877	0.001939576
1.77	0.9204	1.46515	5274540	4854686.616	4.854687	0.001831957
1.88	0.9776	1.469853	5291470.8	5172941.854	5.172942	0.001952054
2.06	1.0712	1.474563	5308426.8	5686386.788	5.686387	0.002145806
2.01	1.0452	1.479283	5325418.8	5566127.73	5.566128	0.002100426
1.83	0.9516	1.50433	5415588	5153473.541	5.153474	0.001944707
2.11	1.0972	1.569685	5650866	6200130.175	6.20013	0.002339672
2.22	1.1544	1.631615	5873814	6780730.882	6.780731	0.002558766
2.39	1.2428	1.70256	6129216	7617389.645	7.61739	0.002874487
2.54	1.3208	1.807704	6507734.4	8595415.596	8.595416	0.003243553
3.71	1.9292	2.055457	7399645.2	14275395.52	14.2754	0.005386942
13.26	6.8952	2.781294	10012658.4	69039282.2	69.03928	0.026052559
26.63	13.8476	4.291121	15448035.6	213918217.8	213.9182	0.080723856

 doi:10.20944/preprints202306.1072.v1

20.42	10.6184	6.396291	23026647.6	244506154.9	244.5062	0.092266474
28.07	14.5964	9.66576	34796736	507907077.4	507.9071	0.191663048
36.36	18.9072	12.059806	43415301.6	820861790.4	820.8618	0.309759166
23.69	12.3188	13.835157	49806565.2	613557115.4	613.5571	0.231530987
16.85	8.762	14.624897	52649629.2	461316051.1	461.3161	0.174081529
12.16	6.3232	14.686552	52871587.2	334317620.2	334.3176	0.126157593
9.24	4.8048	15.209804	54755294.4	263088238.5	263.0882	0.099278581
8	4.16	17.119121	61628835.6	256375956.1	256.376	0.096745644
7.06	3.6712	20.183078	72659080.8	266746017.4	266.746	0.100658875
6.37	3.3124	21.950873	79023142.8	261756258.2	261.7563	0.098775946
6.03	3.1356	21.34665	76847940	240964400.7	240.9644	0.090929963
5.67	2.9484	19.185333	69067198.8	203637728.9	203.6377	0.076844426
5.15	2.678	16.512742	59445871.2	159196043.1	159.196	0.060073979
4.8	2.496	13.829853	49787470.8	124269527.1	124.2695	0.046894161
4.58	2.3816	12.049374	43377746.4	103308440.8	103.3084	0.038984317
4.46	2.3192	10.730926	38631333.6	89593788.89	89.59379	0.033808977
4.08	2.1216	9.847518	35451064.8	75212979.08	75.21298	0.028382256
4.05	2.106	9.021546	32477565.6	68397753.15	68.39775	0.025810473
4.18	2.1736	8.237199	29653916.4	64455752.69	64.45575	0.024322926
3.95	2.054	7.63155	27473580	56430733.32	56.43073	0.021294616
3.66	1.9032	7.079681	25486851.6	48506575.97	48.50658	0.018304368
3.4	1.768	6.622038	23839336.8	42147947.46	42.14795	0.015904886
3.25	1.69	6.245463	22483666.8	37997396.89	37.9974	0.01433864
3.08	1.6016	5.96578	21476808	34397255.69	34.39726	0.012980096
2.95	1.534	5.732923	20638522.8	31659493.98	31.65949	0.011946979
2.78	1.4456	5.521837	19878613.2	28736523.24	28.73652	0.010843971
2.5	1.3	5.292171	19051815.6	24767360.28	24.76736	0.009346174
2.33	1.2116	5.068929	18248144.4	22109451.76	22.10945	0.008343189
2.5	1.3	4.853902	17474047.2	22716261.36	22.71626	0.008572174
2.62	1.3624	4.614081	16610691.6	22630406.24	22.63041	0.008539776
2.41	1.2532	4.414846	15893445.6	19917666.03	19.91767	0.0075161
2.49	1.2948	4.214592	15172531.2	19645393.4	19.64539	0.007413356
2.49	1.2948	4.02859	14502924	18778386	18.77839	0.007086183
2.33	1.2116	3.85956	13894416	16834474.43	16.83447	0.006352632
2.47	1.2844	3.729177	13425037.2	17243117.78	17.24312	0.006506837
2.49	1.2948	3.616494	13019378.4	16857491.15	16.85749	0.006361317
2.24	1.1648	3.515267	12654961.2	14740498.81	14.7405	0.005562452
2.08	1.0816	3.443143	12395314.8	13406772.49	13.40677	0.005059159
2.25	1.17	3.395978	12225520.8	14303859.34	14.30386	0.005397683
2.12	1.1024	3.367167	12121801.2	13363073.64	13.36307	0.005042669
2.17	1.1284	3.376441	12155187.6	13715913.69	13.71591	0.005175816
2.03	1.0556	3.405045	12258162	12939715.81	12.93972	0.004882912
2.07	1.0764	3.467502	12483007.2	13436708.95	13.43671	0.005070456
1.97	1.0244	3.534771	12725175.6	13035669.88	13.03567	0.004919121
1.85	0.962	3.643486	13116549.6	12618120.72	12.61812	0.004761555
1.97	1.0244	3.727272	13418179.2	13745582.77	13.74558	0.005187012
2.33	1.2116	3.795791	13664847.6	16556329.35	16.55633	0.006247671
2.06	1.0712	3.824707	13768945.2	14749294.1	14.74929	0.005565771
2.26	1.1752	3.88128	13972608	16420608.92	16.42061	0.006196456
2.1	1.092	3.915546	14095965.6	15392794.44	15.39279	0.005808602
2.1	1.092	3.901942	14046991.2	15339314.39	15.33931	0.005788421
2.1	1.092	3.888367	13998121.2	15285948.35	15.28595	0.005768282
2.08	1.0816	3.863066	13907037.6	15041851.87	15.04185	0.005676171
2	1.04	3.774092	13586731.2	14130200.45	14.1302	0.005332151
2.06	1.0712	3.648362	13134103.2	14069251.35	14.06925	0.005309151
1.86	0.9672	3.479014	12524450.4	12113648.43	12.11365	0.004571188
1.64	0.8528	3.339059	12020612.4	10251178.25	10.25118	0.003868369

Preprints (www.preprints.org) | NOT PEER-REVIEWED | Posted: 15 June 2023 doi:10.20944/preprints202306.1072.v1

1.9	0.988	3.191403	11489050.8	11351182.19	11.35118	0.004283465
2.11	1.0972	3.080294	11089058.4	12166914.88	12.16691	0.004591289
1.86	0.9672	2.971337	10696813.2	10345957.73	10.34596	0.003904135
1.8	0.936	2.868075	10325070	9664265.52	9.664266	0.003646893
2.24	1.1648	2.775263	9990946.8	11637454.83	11.63745	0.004391492
1.98	1.0296	2.675196	9630705.6	9915774.486	9.915774	0.003741802
2.03	1.0556	2.596988	9349156.8	9868969.918	9.86897	0.00372414
1.99	1.0348	2.517013	9061246.8	9376578.189	9.376578	0.003538331
1.88	0.9776	2.438069	8777048.4	8580442.516	8.580443	0.003237903
1.9	0.988	2.368357	8526085.2	8423772.178	8.423772	0.003178782
1.9	0.988	2.303901	8294043.6	8194515.077	8.194515	0.00309227
1.9	0.988	2.255489	8119760.4	8022323.275	8.022323	0.003027292
1.9	0.988	2.208585	7950906	7855495.128	7.855495	0.002964338

Table A2. Calculation of FSS volume pertaining to different grain sizes at GCDS.

Particle Size (mm)	Mass in g (Bed load)	Mass in g (Total sediment load)	Cumulative Proportion	Absolute Proportion
2			0.260	0.26
1.4	1.01	1.010	0.539	0.28
1	4.96	4.960	1.630	1.09
710um	25.46	25.460	7.292	5.66
500um	161.56	161.560	44.884	37.59
355um	195.14	195.140	54.158	9.27
250um	245.98	245.980	68.201	14.04
180um	252.43	252.430	69.982	1.78
125um	252.53	252.530	70.010	0.03
90um	252.54	252.540	70.013	0.00
63um	252.55	317.04 (252.55+64.49)	87.829	17.82
<63um	252.57	361.11 (252.57+44.045)	100.000	12.17
Proportion of particles above 2 mm in size is taken as 0.26				

Table A3. Absolute proportions of sediments pertaining to corresponding particle sizes.

Particle size in m (Input in CAESAR-Lisflood is in m)	Absolute Proportions
0.000063	12.17
0.000125	17.82
0.00025	1.81
0.0005	23.32
0.001	43.25
0.002	1.37
0.004	0.26
0.008	0
0.032	0

Total sediment=1.28*Bedload^1.02=1.28*252.57^1.02=361.1099g
Suspended sand +suspended mud = 361.1099-252.57=108.54g
Suspended sand: suspended mud = 41:28
Suspended sand=64.49478g
Suspended mud=44.04522g

Preprints (www.preprints.org) | NOT PEER-REVIEWED | Posted: 15 June 2023 doi:10.20944/preprints202306.1072.v1

Table A4. Hourly input at GCUS - Volume of sediments (m^3) of corresponding grain sizes in m (shown in first row).

0.08	0.032	0.04	0.02	0.01	0.0005	0.00025	0.000125	0.000063
0	0	4.74E-05	0.0002497	0.007881333	0.00425	0.00033	0.003247291	0.002218
0	0	4.70E-05	0.0002475	0.0078147	0.004214	0.000327	0.003219837	0.002199
0	0	4.54E-05	0.0002392	0.007549936	0.004071	0.000316	0.003110748	0.002124
0	0	4.43E-05	0.0002333	0.007364627	0.003971	0.000308	0.003034397	0.002072
0	0	4.41E-05	0.0002323	0.007335073	0.003955	0.000307	0.00302222	0.002064
0	0	4.24E-05	0.0002235	0.007055371	0.003804	0.000295	0.002906976	0.001985
0	0	4.20E-05	0.0002215	0.006991993	0.00377	0.000293	0.002880863	0.001967
0	0	4.26E-05	0.0002246	0.007091732	0.003824	0.000297	0.002921958	0.001996
0	0	3.99E-05	0.0002104	0.006641619	0.003581	0.000278	0.002736501	0.001869
0	0	4.11E-05	0.0002165	0.006834071	0.003685	0.000286	0.002815795	0.001923
0	0	4.14E-05	0.0002184	0.006894305	0.003717	0.000289	0.002840613	0.00194
0	0	4.15E-05	0.0002189	0.006910662	0.003726	0.000289	0.002847353	0.001945
0	0	3.75E-05	0.0001976	0.006238513	0.003364	0.000261	0.002570412	0.001755
0	0	4.14E-05	0.0002183	0.006892907	0.003717	0.000288	0.002840037	0.00194
0	0	3.91E-05	0.0002062	0.006510448	0.00351	0.000272	0.002682455	0.001832
0	0	4.17E-05	0.0002197	0.006937249	0.003741	0.00029	0.002858307	0.001952
0	0	4.58E-05	0.0002416	0.007625811	0.004112	0.000319	0.003142011	0.002146
0	0	4.49E-05	0.0002364	0.007464536	0.004025	0.000312	0.003075561	0.0021
0	0	4.15E-05	0.0002189	0.00691114	0.003726	0.000289	0.00284755	0.001945
0	0	5.00E-05	0.0002634	0.008314774	0.004483	0.000348	0.003425879	0.00234
0	0	5.47E-05	0.000288	0.009093397	0.004903	0.000381	0.00374669	0.002559
0	0	6.14E-05	0.0003236	0.010215411	0.005508	0.000428	0.004208985	0.002874
0	0	6.93E-05	0.0003651	0.011527007	0.006215	0.000482	0.004749393	0.003244
0	0	0.0001151	0.0006064	0.019144226	0.010322	0.000801	0.007887864	0.005387
0	0	0.0005566	0.0029328	0.092586129	0.049922	0.003875	0.038147626	0.026053
0	0	0.0017246	0.0090872	0.286878123	0.154682	0.012006	0.11820042	0.080724
0	0	0.0019712	0.0103866	0.327898519	0.1768	0.013722	0.135101771	0.092266
0	0	0.0040947	0.0215759	0.68113614	0.367262	0.028505	0.280643839	0.191663
0	0	0.0066177	0.0348702	1.10082859	0.593557	0.046069	0.453566832	0.309759
0	0	0.0049464	0.0260639	0.822819654	0.443657	0.034435	0.339020722	0.231531
0	0	0.0037191	0.0195967	0.61865457	0.333573	0.025891	0.254899987	0.174082
0	0	0.0026952	0.0142018	0.448341485	0.241742	0.018763	0.184727058	0.126158
0	0	0.002121	0.011176	0.352818292	0.190236	0.014765	0.145369294	0.099279
0	0	0.0020669	0.0108908	0.343816688	0.185383	0.014389	0.141660425	0.096746
0	0	0.0021505	0.0113314	0.357723609	0.192881	0.014971	0.147390398	0.100659
0	0	0.0021103	0.0111194	0.35103202	0.189273	0.014691	0.144633309	0.098776
0	0	0.0019426	0.0102362	0.323148799	0.174239	0.013524	0.133144777	0.09093
0	0	0.0016417	0.0086505	0.273091325	0.147248	0.011429	0.11251994	0.076844
0	0	0.0012834	0.0067626	0.213492159	0.115113	0.008935	0.087963706	0.060074
0	0	0.0010018	0.005279	0.166653449	0.089858	0.006974	0.068665074	0.046894
0	0	0.0008329	0.0043885	0.13854328	0.074701	0.005798	0.057083035	0.038984
0	0	0.0007223	0.0038059	0.120151048	0.064784	0.005028	0.04950501	0.033809
0	0	0.0006064	0.003195	0.100865455	0.054386	0.004221	0.041558899	0.028382
0	0	0.0005514	0.0029055	0.091725797	0.049458	0.003839	0.037793149	0.02581
0	0	0.0005196	0.0027381	0.08643932	0.046607	0.003617	0.035614999	0.024323
0	0	0.0004549	0.0023972	0.075677252	0.040804	0.003167	0.031180778	0.021295
0	0	0.0003911	0.0020606	0.065050446	0.035075	0.002722	0.026802288	0.018304
0	0	0.0003398	0.0017904	0.056523115	0.030477	0.002365	0.02328883	0.015905
0	0	0.0003063	0.0016141	0.050956959	0.027476	0.002133	0.020995445	0.014339
0	0	0.0002773	0.0014612	0.046128938	0.024872	0.00193	0.019006189	0.01298
0	0	0.0002552	0.0013449	0.042457423	0.022893	0.001777	0.01749344	0.011947
0	0	0.0002317	0.0012207	0.038537531	0.020779	0.001613	0.015878354	0.010844
0	0	0.0001997	0.0010521	0.033214627	0.017909	0.00139	0.013685194	0.009346

0	0	0.0001782	0.0009392	0.0296502	0.015987	0.001241	0.012216568	0.008343
0	0	0.0001831	0.000965	0.030463971	0.016426	0.001275	0.012551861	0.008572
0	0	0.0001824	0.0009613	0.030348834	0.016364	0.00127	0.012504421	0.00854
0	0	0.0001606	0.0008461	0.026710874	0.014402	0.001118	0.011005498	0.007516
0	0	0.0001584	0.0008345	0.026345739	0.014205	0.001103	0.010855054	0.007413
0	0	0.0001514	0.0007977	0.025183026	0.013578	0.001054	0.010375989	0.007086
0	0	0.0001357	0.0007151	0.022576116	0.012173	0.000945	0.009301882	0.006353
0	0	0.000139	0.0007325	0.023124133	0.012468	0.000968	0.009527677	0.006507
0	0	0.0001359	0.0007161	0.022606983	0.012189	0.000946	0.0093146	0.006361
0	0	0.0001188	0.0006262	0.019767959	0.010659	0.000827	0.008144856	0.005562
0	0	0.0001081	0.0005695	0.017979346	0.009694	0.000752	0.007407906	0.005059
0	0	0.0001153	0.0006076	0.019182398	0.010343	0.000803	0.007903591	0.005398
0	0	0.0001077	0.0005677	0.017920743	0.009663	0.00075	0.007383761	0.005043
0	0	0.0001106	0.0005827	0.018393925	0.009918	0.00077	0.007578722	0.005176
0	0	0.0001043	0.0005497	0.017352993	0.009357	0.000726	0.007149834	0.004883
0	0	0.0001083	0.0005708	0.018019493	0.009716	0.000754	0.007424448	0.00507
0	0	0.0001051	0.0005538	0.017481674	0.009426	0.000732	0.007202854	0.004919
0	0	0.0001017	0.000536	0.016921713	0.009124	0.000708	0.006972137	0.004762
0	0	0.0001108	0.0005839	0.018433713	0.009939	0.000771	0.007595116	0.005187
0	0	0.0001335	0.0007033	0.022203105	0.011972	0.000929	0.009148193	0.006248
0	0	0.0001189	0.0006265	0.019779754	0.010665	0.000828	0.008149716	0.005566
0	0	0.0001324	0.0006975	0.022021095	0.011874	0.000922	0.0090732	0.006196
0	0	0.0001241	0.0006539	0.02064273	0.01113	0.000864	0.008505282	0.005809
0	0	0.0001237	0.0006516	0.02057101	0.011092	0.000861	0.008475732	0.005788
0	0	0.0001232	0.0006493	0.020499442	0.011053	0.000858	0.008446244	0.005768
0	0	0.0001213	0.000639	0.020172093	0.010877	0.000844	0.008311369	0.005676
0	0	0.0001139	0.0006003	0.01894951	0.010217	0.000793	0.007807636	0.005332
0	0	0.0001134	0.0005977	0.018867773	0.010173	0.00079	0.007773959	0.005309
0	0	9.77E-05	0.0005146	0.016245184	0.008759	0.00068	0.006693391	0.004571
0	0	8.26E-05	0.0004355	0.013747491	0.007413	0.000575	0.005664284	0.003868
0	0	9.15E-05	0.0004822	0.015222667	0.008208	0.000637	0.006272091	0.004283
0	0	9.81E-05	0.0005169	0.016316617	0.008798	0.000683	0.006722824	0.004591
0	0	8.34E-05	0.0004395	0.013874596	0.007481	0.000581	0.005716655	0.003904
0	0	7.79E-05	0.0004105	0.012960403	0.006988	0.000542	0.005339986	0.003647
0	0	9.38E-05	0.0004944	0.015606577	0.008415	0.000653	0.006430271	0.004391
0	0	7.99E-05	0.0004212	0.013297693	0.00717	0.000557	0.005478957	0.003742
0	0	7.96E-05	0.0004192	0.013234925	0.007136	0.000554	0.005453095	0.003724
0	0	7.56E-05	0.0003983	0.012574596	0.00678	0.000526	0.005181024	0.003538
0	0	6.92E-05	0.0003645	0.011506927	0.006204	0.000482	0.00474112	0.003238
0	0	6.79E-05	0.0003578	0.011296822	0.006091	0.000473	0.004654552	0.003179
0	0	6.61E-05	0.0003481	0.010989373	0.005925	0.00046	0.004527876	0.003092
0	0	6.47E-05	0.0003408	0.010758453	0.005801	0.00045	0.004432731	0.003027
0	0	6.33E-05	0.0003337	0.010534725	0.00568	0.000441	0.00434055	0.002964

References

1. Hancock, G., D. Verdon-Kidd, and J. Lowry, *Sediment output from a post-mining catchment–Centennial impacts using stochastically generated rainfall.* Journal of Hydrology, 2017. **544**: p. 180-194.
2. Nair, D., et al., *Stream Suspended Mud as an Indicator of Post-Mining Landform Stability in Tropical Northern Australia.* Water, 2021. **13**(22): p. 3172.
3. Nair, D., S.M. Bellairs, and K. Evans, *An approach to simulate long-term erosion equilibrium of a rehabilitated mine landform*, in *Mine Closure 2022: 15th International Conference on Mine Closure*, M.T. A.B. Fourie and G. Boggs, Editors. 2022, Australian Centre for Geomechanics: Brisbane. p. 1063-1074.

4. Lowry, J.B.C., et al., *Assessing soil erosion on a rehabilitated landform using the CAESAR landscape evolution model ©*, in *Mine Closure 2011: Proceedings of the Sixth International Conference on Mine Closure*, M.T. A.B. Fourie and A. Beersing, Editors. 2011, Australian Centre for Geomechanics: Alberta. p. 613-621.
5. Australian Government. *Closure and Rehabilitation Process of the Ranger Uranium Mine.Australian Government.Department of Agriculture,Water and Environment.* 2020; Available from: https://www.environment.gov.au/science/supervising-scientist/ranger-mine/closure-rehabilitation.
6. East, T.J., *Landform evolution*, in *Landscape and vegetation ecology of the Kakadu Region, northern Australia*, C.M. Finlayson. and I. Oertzen., Editors. 1996, Springer. p. 37-55.
7. Bureau of Meteorology. *Annual Climate Statement 2019, Australian Government*. 2020.
8. Lowry, J., et al., *Understanding post-mining landforms: Utilising pre-mine geomorphology to improve rehabilitation outcomes.* Geomorphology, 2019. **328**: p. 93-107.
9. Erskine, W. and M. Saynor, *Assessment of the off-site geomorphic impacts of uranium mining on Magela Creek, Northern Territory, Australia. Supervising Scientist Report 156. Supervising Scientist, Darwin.* 2000.
10. Tucker, G.E. and G.R. Hancock, *Modelling landscape evolution.* Earth Surface Processes and Landforms, 2010. **35**(1): p. 28-50.
11. Evans, K., T. Aspinall, and L. Bell. *Erosion prediction models and factors affecting the application of the Universal Soil Loss Equation to post-mining landscapes in Central Queensland*. in *Queensland Coal Symposium, Brisbane, Aust, 08/29-30/91*. 1991.
12. Evans, K.G., *Determination of interrill erodibility parameters for selected overburden spoil types from Central Queensland open-cut coal mines*. 1992: University of Queensland.
13. Kirkby, M., *Hillslope process-response models based on the continuity equation.* Institute of British Geographers Serial Publication 1971. **3**(1): p. 5-30.
14. Willgoose, G., R. Bras, and I. Rodriguez-Iturbe. *Modelling of the Erosional Impacts of Landuse Change: A New Approach Using a Physically Based Catchment Evolution Model*. in *Hydrology and Water Resources Symposium 1989: Comparisons in Austral Hydrology; Preprints of Papers*. 1989. Institution of Engineers, Australia.
15. Coulthard, T.J., *Landscape evolution models: a software review.* Hydrological processes, 2001. **15**(1): p. 165-173.
16. Coulthard, T., *Simulating upland river catchment and alluvial fan evolution.* Earth Surface Processes and Landforms, 2002. **27**: p. 269-288.
17. Coulthard, T., M. Kirkby, and M. Macklin, *Modelling geomorphic response to environmental change in an upland catchment.* Hydrological processes, 2000. **14**(11‐12): p. 2031-2045.
18. Beven, K.J. and M.J. Kirkby, *A physically based, variable contributing area model of basin hydrology/Un modèle à base physique de zone d'appel variable de l'hydrologie du bassin versant.* Hydrological Sciences Journal, 1979. **24**(1): p. 43-69.
19. Bates, P.D., M.S. Horritt, and T.J. Fewtrell, *A simple inertial formulation of the shallow water equations for efficient two-dimensional flood inundation modelling.* Journal of Hydrology, 2010. **387**(1-2): p. 33-45.
20. Einstein, H.A., *The bed-load function for sediment transportation in open channel flows*. 1950: US Government Printing Office.
21. Wilcock, P.R. and J.C. Crowe, *Surface-based transport model for mixed-size sediment.* Journal of Hydraulic Engineering, 2003. **129**(2): p. 120-128.
22. Evans, K., *Assessment of broader catchment surface water impacts of redevelopment of the Rustler's Roost mine and Quest 19 mining precinct*. 2022.
23. Meteorology, B.o. *Evaporation: Average Monthly & Annual Evaporation*. 2006 [cited 2023 13/06/2023]; Available from: http://www.bom.gov.au/watl/evaporation/.
24. QGIS Development Team. *QGIS Geographic Information System. Open Source Geospatial Foundation Project.* 2022; Available from: https://qgis.osgeo.org.

25. Moliere, D., M. Saynor, and K. Evans, *Suspended sediment concentration-turbidity relationships for Ngarradj - a seasonal stream in the wet-dry tropics.* Australasian Journal of Water Resources, 2005. **9**(1): p. 37-48.
26. Saynor, M.J. and K.G. Evans, *Sediment loss from a waste rock dump, ERA Ranger Mine, Northern Australia.* Australian Geographical Studies, 2001. **39**(1): p. 34-51.
27. Evans, K., et al., *Baseline suspended-sediment, solute, EC and turbidity characteristics for the Ngarradj catchment, Northern Territory, and the impact of mine construction.* Supervising Scientist Report, 2004(SSR179): p. 1-75.
28. Manning, R., *On the flow of water in open channels and pipes: Institute of Civil Engineers of Ireland Transactions, v. 20.* 1891.
29. Chow, V.T., *Open-channel hydraulics. Caldwell*. 1959: New Jersey, USA: The Blackburn Press.
30. Bureau of Meteorology, A.G. *Northern Territory in February 2011: Darwin Airport smashes rainfall records*. 2011 [cited 2021 17/06/2021]; Available from: http://www.bom.gov.au/climate/current/month/nt/archive/201102.summary.shtml.
31. EnviroConsult Australia Pty Ltd, *Existing hydrological condition and hydrology model calibration, Grants Lithium Project EIS*. 2018. p. 59.
32. Hutley, L., A. O'grady, and D. Eamus, *Evapotranspiration from Eucalypt open - forest savanna of Northern Australia.* Functional Ecology, 2000. **14**(2): p. 183-194.